Chemical Physics Letters 498 (2010) 334–337

Contents lists available at ScienceDirect

Chemical Physics Letters

journal homepage: www.elsevier.com/locate/cplett

Graphene nanomeshes: Onset of conduction band gaps

Kenneth Lopata, Ryan Thorpe, Shlomi Pistinner, Xiangfeng Duan, Daniel Neuhauser *

Department of Chemistry and Biochemistry, UCLA, Los Angeles, CA 90095-1569, United States

ARTICLE INFO

Article history:
Received 22 June 2010
In final form 31 August 2010
Available online 16 September 2010

ABSTRACT

Hückel simulations of large finite graphene nanomeshes with lithographically induced holes show sizable band gaps in the conduction while the optical absorption has generally the same semi-metal character as pure graphene. There is a strong dependence of the band gap on the angle between the graphene axis and the periodic hole axis. Simple modification of on-site energies shows that substituents on the edges of the holes could also have a significant effect. These simulations show that graphene nanomeshes, which have been recently fabricated, are potentially useful tunable materials for electronic applications.

© 2010 Elsevier B.V. All rights reserved.

Graphene as a new electronic material has been extensively investigated lately both experimentally and theoretically [1–7]. Graphene itself is a semi-metal [8] but semiconducting behavior is often desired. A potential advantage of graphene over carbon nanotubes is that the two-dimensional (2D) nature of graphene could lead to large scale integration without sophisticated assembly steps [9,10]. 1D-like graphene nanoribbons show a width-tunable band gap [11–16], but are harder to assemble than inherently 2D structures.

Interestingly, recently a new type of graphene structure, nanomeshes (also known as antidot lattices), were produced, with periodic holes carved out using electron beam lithography [5] or a block co-polymer template [17] (Figure 1). The nanomesh structure introduces finite size effects into a large sheet of graphene while retaining the overall 2D nature, resulting in ferromagnetism [18] or interesting band-structure-like transmission which depends on the holes' periodic arrangement. Gaps in the conduction (i.e., very low transmission over a range of energies) were observed experimentally for nanomeshes with periodicities on the order of 100 nm [5], as well as theoretically using periodic tight-binding [6] and density-functional theory (DFT) simulations [7].

Here we simulate large finite nanomeshes with small (< 10 nm diameter) holes, corresponding to recently synthesized systems [17]. We demonstrate that these meshes exhibit very large tunable transmission gaps (few meV to >1 eV), despite a finite density of states around $E = 0$.

We use a typical Hückel Hamiltonian [19,20] on a hexagonal honeycomb arrangement (Figure 1), which captures the semi-metal effects of graphene without electron-polarization:

$$H_{ij} = \begin{cases} \alpha_j & \text{if } i = j, \\ \beta & \text{if } i \neq j,\ i,\ j \text{ nearest neighbors}, \\ 0 & \text{otherwise} \end{cases} \quad (1)$$

where $\beta = 2.7$ eV [21]. Typically we use a 212 nm $\times$ 212 nm lattice, with about 1.7 million grid points. An alternate more accurate approach is a semiempirical method involving polarization, for example the Pariser–Parr–Pople (PPP) approximation [22]. PPP, however, is an iterative method and moreover the density is required at each point is required for transmission calculations, making PPP calculations unfeasible for systems this large (up to millions of points) without further approximations. Carving the nanomesh excludes sites within the diameter of each hole (Figure 1), resulting in a strictly non-commensurate lattice.

The transmission probability per unit bond is obtained from a trace approach [23]:

$$P(E) = \frac{N(E)}{N_y} = \frac{4}{N_y}\mathrm{Tr}\left[\Gamma_L G^\dagger \Gamma_R G\right] = \frac{4}{N_y}\mathrm{Tr}\left[A^\dagger(E)A(E)\right]. \quad (2)$$

Here, $A \equiv \Gamma_L^{\frac{1}{2}} G \Gamma_R^{\frac{1}{2}}$, and we introduced the transmission sum, $P(E)$. The Green's function is defined as:

$$G = (E - (H - i\Gamma_L - i\Gamma_R))^{-1}, \quad (3)$$

including left- and right-absorbing potentials, Γ_L, Γ_R, chosen to be parabolic and typically extending over 15–20 bonds, with maximum height taken to be β. The results are insensitive to the precise absorbing potential form and parameters [24].

In essence, Eq. (2) computes the flux of a wavefunction with energy E originating in the left region containing an absorbing potential Γ_L that is absorbed by the right region containing absorbing potential Γ_R. The number of channels for the probability flux is essentially equal to (up to spin factors) N_y, the number of atoms along the direction perpendicular to the transmission; the sum is therefore divided by N_y such that $P(E)$ is normalized to a "per

* Corresponding author. Fax: + 1 310 267 0319.
E-mail address: dxn@chem.ucla.edu (D. Neuhauser).

0009-2614/$ - see front matter © 2010 Elsevier B.V. All rights reserved.
doi:10.1016/j.cplett.2010.08.086

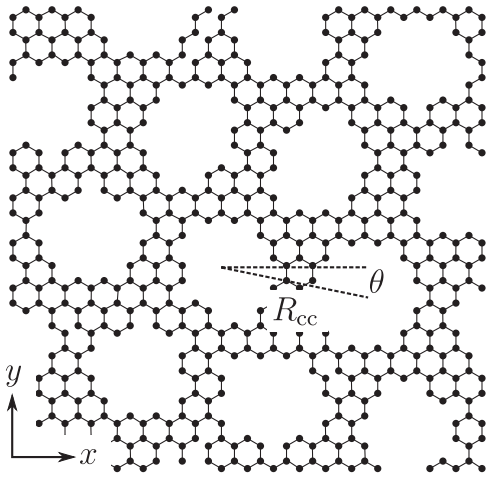

Figure 1. Schematic graphene nanomesh with a hexagonal array of holes with periodicity R_{cc}, and oriented at an angle θ to the carbon lattice. For clarity, in this figure the holes are quite small and appear disordered; the actual simulated nanomeshes had much larger holes with no disorder.

channel" probability (i.e., ranges between 0 and 1). This trace formulation is often used in reactive scattering wavepacket calculations and simulations of electron transport through molecular systems (see review in Ref. [25] and further examples in Refs. [26,27].)

The action of $G(E)$ for a large system is challenging. For this, first cast the trace as:

$$P(E) = \frac{4}{N_y}\frac{N_{\text{grid}}}{N_\Psi}\sum_\Psi \langle \Psi | A^\dagger(E) A(E) | \Psi \rangle, \tag{4}$$

where each Ψ is a different orthonormal initial wavefunction. Formally the sum needs to extend over all possible wavefunctions, but it was sufficient here to use a single wavefunction $N_\Psi = 1$, with a random value between -1 and 1 at each grid point. This approximation is valid because the large number of atoms results in good statistics, and each term is positive definite so there are no cancellations. We checked that $N_\Psi = 5$ yields essentially identical results.

To act $G(E)$ on Ψ we use the time-dependent Chebyshev method [28]; defining $|\chi\rangle \equiv \Gamma_R^{\frac{1}{2}}|\Psi\rangle$,

$$\begin{aligned} iG|\chi \cong & \int_0^T e^{i(E-H+i\Gamma_L+i\Gamma_R)t}|\chi \mathrm{d}t \\ = & \sum_{k=0}^{T/\tau-1} e^{iEk\tau}\int_0^\tau e^{i(E-H+i\Gamma_L+i\Gamma_R)t}|\chi(k\tau)\mathrm{d}t \\ = & \sum_{k=0}^{T/\tau-1} e^{iEk\tau}\sum_n a_n(E)C_n(H-i\Gamma_L-i\Gamma_R)|\chi(k\tau), \end{aligned} \tag{5}$$

where T is a large time by which $\chi(T)$ decays to zero, and we introduced the Chebyshev polynomials, C_n, acting on a shifted Hamiltonian divided by a spectral width, ΔH. The intermediate time step-size, taken here as $100/\Delta H$, is needed since a Chebyshev expansion loses stability if used for more than a few hundred terms at a time for a Hamiltonian with absorbing potentials. The time dependent wavefunction is analogous:

$$|\chi([k+1]\tau) = \sum_n b_n C_n(H - i\Gamma_L - i\Gamma_R)|\chi(k\tau)\rangle. \tag{6}$$

Finally, a_n and b_n are Chebyshev coefficients for $\int_0^\tau e^{i(E-H+i\Gamma_L+i\Gamma_R)t}\mathrm{d}t$ and $e^{-(H-i\Gamma_L-i\Gamma_R)\tau}$.

The resulting method is very stable and robust, with minimal storage requirements as each $A(E)|\Psi$ is only collected in the small grid region where Γ_L is non-zero. For all the (non-optimized) simulations $T = 500$ fs, requiring about 10^4 Chebyshev terms. Most simulations were done with identical on-site energy (equaling the Fermi energy), taken for simplicity as $\alpha_i = 0$.

Figure 2a shows $P(E)$ for different holes diameters, keeping the periodicity (hole-to-hole distance) fixed at 8 nm. Fabricating meshes with holes of this size will be experimentally feasible in the near future. A clear insulating band develops around zero energy as the hole diameter is increased; the transmission is not step-like due to the finite system size. To quantify the insulating band, we define a "conduction-onset" as the energy where the transmission first reaches $P(E) = 0.001$. Note that in graphene $|E| \gtrsim 1$ eV would require non-physical densities (i.e. complete depletion of charge), meaning systems with a conduction onset beyond 1 eV will effectively become insulators. We nevertheless present results in the > 1 eV regime for illustrative purposes.

Figure 2b illustrates that the observed conduction onset is not due to intrinsic band gap formation, but is a purely transmission-based effect. Specifically, we calculated the average density of the states (DOS) using a Chebyshev approach (geared to Hermitian Hamiltonians) for the delta function:

$$n(E) \equiv \mathrm{Tr}[\delta(E-H)] = \frac{1}{N_\Psi}\sum_\Psi g_n \langle \Psi | C_n(H) | \Psi \rangle, \tag{7}$$

where g_n are the coefficients of a single (many-term) Chebyshev expansion of a narrow delta-function-like Gaussian; as Figure 2b shows, there is no band gap in $n(E)$ even though the conduction is gapped. Physically, the non-zero DOS around $E = 0$ arises from edge states around the boundaries of the holes. In practice these states would be disrupted by the presence of terminal capping atoms (e.g., hydrogen); regardless, they are localized and play no role in transmission.

Figure 3 shows that the conduction onset is mainly dependent on the neck width, i.e. the difference $R_{cc} - d$ between the hole-to-hole distance and the diameter. Here, we studied four systems with

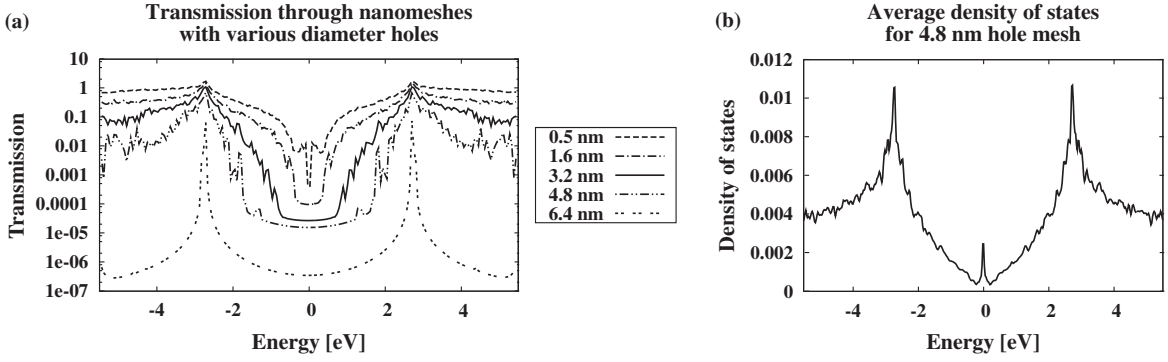

Figure 2. (a) Transmission $P(E)$ through a 212 nm × 212 nm graphene nanomesh as a function of hole diameter. With increasing hole diameter an insulating band develops, shown by a flat region around zero energy. The hole-to-hole separation here is 8 nm. (b) Similar to (a), but for the average density of states and a hole diameter of 4.8 nm; unlike the transmission, no band gap emerges in the density of states.

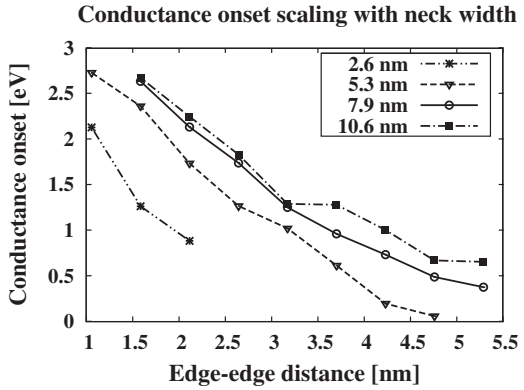

Figure 3. Conduction onset for a hexagonal grid, taken as the start of the region near the Fermi energy where $P(E) < 0.001$, as a function of neck width (minimum distance between nearest-neighbor hole edges). Different periodicities (R_{cc}) are denoted by distinct lines; the results show a roughly general inverse dependence on the neck width.

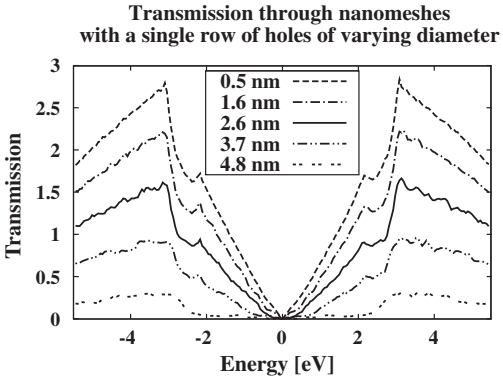

Figure 5. Similar to Figure 2(a) with just one set of holes (perpendicular to the transmission direction) with periodicity of 8 nm; the figure shows that the conduction onset requires a periodic arrangement along the transmission direction rather than a single restriction.

different R_{cc} values and varied the hole diameters to adjust the neck width; all four systems show a similar inverse relationship between neck width and conduction onset. Narrower neck widths give smaller channels for the electrons to travel through, leading to a more pronounced insulating band. It is known that edge effects in graphene ribbons dominate the transport properties and the electronic wavefunction is highly localized around the edge [11]. Additionally, tight-binding simulations of imperfect wedge-shaped constrictions in ribbons have shown transmission gaps of $\simeq 1$ eV for constrictions a few atoms wide, despite a large DOS around $E = 0$ [29]. In essence, a nanomesh is a periodic arrangement of constrictions. Low energy states in the nanomesh are localized around the hole edges and decoupled from the electrodes so they play no role in transmission. Narrower neck widths amplify this effect, so even large holes and large diameters show sizable increases in conduction onset.

Strictly, the nanomesh is insulating as the transmission decreases with total system length. In practice, however, beyond the 200 nm system size we studied (and depending on temperature, possibly even below) dephasing will occur so the system will conduct by hopping, and the lack of metallic character will be immaterial for conduction. Additionally, both the transmission and DOS are independent of system width beyond 30 nm.

An interesting aspect, covered in Figure 4, is the dependence of the conduction onset on the angle θ between the hexagonal underlying carbon atom grid and the hexagonal hole grids. Although the two grids are very different in scale, there is an almost step-like dependence of the onset on the angle between the grids. A simple interpretation is that matched lattices allow for delocalized electronic states across the entire system and thus high conductivity (low conduction onset), while lattice mismatches frustrate the delocalization.

In Figure 5 we compare the 2D geometry studied above to a system with a single perpendicular row of holes, which shows no conduction gap. The conduction onset delay is thus due to the periodicity of the holes. It is analogous to Anderson localization near the Fermi energy [30,31] and can be viewed as creation of a meta-material. We also note in passing that an analogous system to nanomeshes is narrow nanoribbons, which in density functional theory simulations also show semiconducting behavior for narrow neck widths [13] due to the angle between the underlying grid and the nanoribbon, while for nanomeshes the effect is due to the underlying periodicity of the 2D mesh structure.

The final simulation tackles possible chemical effects on nanomeshes by assigning a parameter $\alpha_{surface}$ to the on-site energies of surface atoms (i.e., on hole edges). Variation of $\alpha_{surface}$ simulates the effects of surface substituents, from, e.g., hydrogen terminated surfaces to those with higher or lower electronegativity. Values of $\alpha_{surface}$ that are less than -1.5 eV or greater than 1.5 eV lead to significant variation in the conductance onset, as

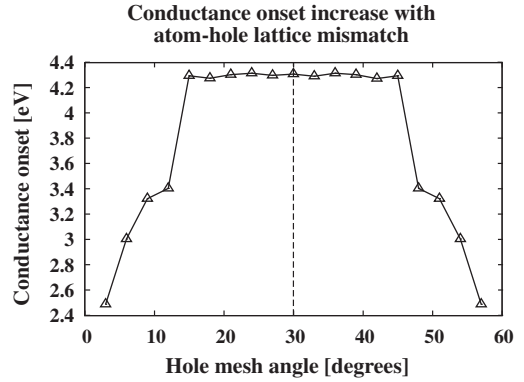

Figure 4. Dependence of the conduction onset on the angle between the axis of the hexagonal graphene and hole grids. A 30° angle, corresponding to the maximum mismatch between the two hexagonal grids, leads to a strongly delayed conduction onset due to frustrated delocalization of the wavefunction.

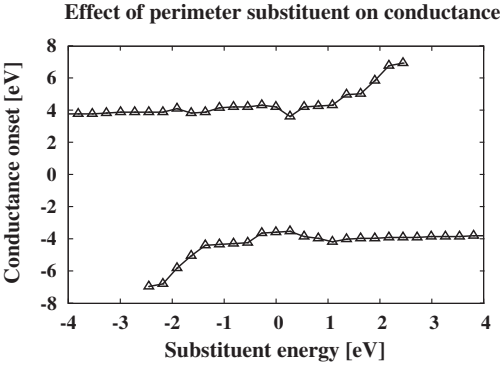

Figure 6. Conduction onset as a function of the local energy of the surface sites (bordering holes), simulating the effect of different substituents. The onset is significantly extended for surface energies with magnitudes greater than 1.5 eV, suggesting transport properties of nanomeshes can be tuned via functionalization of the hole edges.

shown in Figure 6. Nanomesh properties could therefore be tunable by changing surface substituents.

Finally, in real systems the carbon atoms at the hole edges will reorganize to minimize the energy, potentially giving rise to holes with slightly different atomic-level shapes than just exclusion any atom within a hole's radius. To examine the effect of the edge shape on transmission, two systems ($\theta = 0$ and $\theta = 90^\circ$ from Figure 4) were "annealed" so that edges had no dangling carbon atoms (atoms with only one neighbor). The presence or absence of these dangling atoms had no significant effect on the transmission, DOS, or the conduction onset, confirming that the dominant mechanism is just the constriction between holes, which is insensitive to the exact shape of the edges.

In conclusions, large-scale Hückel simulations point to a wealth of controllability of coherent graphene conduction in recently-fabricated nanomeshes through both geometric and lithographic effects and potentially chemical substituents. Due to the two different length scales, conductivity is essentially "gapped" even though the DOS is unchanged. Potential applications abound due to the favorable chemical, structural, and electronic properties of 2D graphene sheets. Further computational studies will elucidate how polarization effects in higher level approaches, such as density-functional theory, will affect the nanomeshes, as well as effects of lattice vibrations on the conduction coherence, and experimental or induced disorder and molecular rearrangements.

Acknowledgments

We are grateful to Nicholas Kiousis for useful discussions and to the NSF for support.

References

[1] K.S. Novoselov, A.K. Geim, S.V. Morozov, D. Jiang, Y. Zhang, S.V. Dubonos, I.V. Grigorieva, A.A. Firsov, Science 306 (2004) 666.
[2] J.S. Bunch, Y. Yaish, M. Brink, K. Bolotin, P.L. McEuen, Nano Lett. 5 (2005) 287.
[3] Y. Zhang, Y.-W. Tan, H.L. Stormer, P. Kim, Nature 438 (2005) 201.
[4] C. Berger, Z. Song, X. Li, X. Wu, N. Brown, C. Naud, D. Mayou, T. Li, J. Hass, A.N. Marchenkov, E.H. Conrad, P.N. First, W.A. de Heer, Science 312 (2006) 1191.
[5] J. Eroms, D. Weiss, New J. Phys. 11 (2009) 095021.
[6] T.G. Pedersen, C. Flindt, J. Pedersen, N.A. Mortensen, A.-P. Jauho, K. Pedersen, Phys. Rev. Lett. 100 (2008) 136804.
[7] J.A. Fürst, J.G. Pedersen, C. Flindt, N.A. Mortensen, M. Brandbyge, T.G. Pedersen, A.-P. Jauho, New J. Phys. 11 (2009) 095020.
[8] K.S. Novoselov, A.K. Geim, S.V. Morozov, D. Jiang, M.I. Katsnelson, I.V. Grigorieva, S.V. Dubonos, A.A. Firsov, Nature 438 (2005) 197.
[9] Y. Huang, X. Duan, Q. Wei, C.M. Lieber, Science 291 (2001) 630.
[10] X. Duan, MRS Bull. 32 (2007) 134.
[11] K. Nakada, M. Fujita, G. Dresselhaus, M.S. Dresselhaus, Phys. Rev. B 54 (1996) 17954.
[12] Y.-W. Son, M.L. Cohen, S.G. Louie, Phys. Rev. Lett. 97 (2006) 216803.
[13] V. Barone, O. Hod, G.E. Scuseria, Nano Lett. 6 (2006) 2748.
[14] T.C. Li, S.-P. Lu, Phys. Rev. B 77 (2008) 085408.
[15] M.Y. Han, B. Özyilmaz, Y. Zhang, P. Kim, Phys. Rev. Lett. 98 (2007) 206805.
[16] J. Bai, X. Duan, Y. Huang, Nano Lett. 9 (2009) 2083.
[17] J. Bai, X. Zhong, S. Jiang, Y. Huang, X. Duan, Nat. Nano. 5 (2010) 190.
[18] N. Shima, H. Aoki, Phys. Rev. Lett. 71 (1993) 4389.
[19] S.K. Maiti, Solid State Commun. 149 (2009) 973.
[20] H. Raza, E. Kan, J. Comp. Electron. 7 (2008) 372.
[21] R. Baer, D. Neuhauser, J. Am. Chem. Soc. 124 (2002) 4200.
[22] S. Evangelisti, G. Bendazzoli, Chem. Phys. Lett. 196 (1992) 511.
[23] T. Seideman, W.H. Miller, J. Chem. Phys. 97 (1992) 2499.
[24] D. Neuhauser, M. Baer, J. Chem. Phys. 90 (1989) 4351.
[25] A. Nitzan, Annu. Rev. Phys. Chem. 52 (2001) 681.
[26] D. Neuhauser, K. Lopata, J. Chem. Phys. 127 (2007) 154715.
[27] D. Walter, D. Neuhauser, R. Baer, Chem. Phys. 229 (2004) 139.
[28] R. Kosloff, J. Phys. Chem. 92 (1998) 2087.
[29] F. Muñoz Rojas, D. Jacob, J. Fernández-Rossier, J.J. Palacios, Phys. Rev. B 74 (2006) 195417.
[30] P.W. Anderson, Phys. Rev. 109 (1958) 1492.
[31] S.-J. Xiong, Y. Xiong, Phys. Rev. B 76 (2007) 214204.